Rovibrational Motion of CO in Solid C_{60}

I. Holleman, G. von Helden, E. H. T. Olthof, P. J. M. van Bentum, R. Engeln, G. H. Nachtegaal, A. P. M. Kentgens, B. H. Meier, A. van der Avoird, and G. Meijer

Research Institute for Materials and Nijmegen SON Research Center, University of Nijmegen, Toernooiveld, NL-6525 ED Nijmegen, The Netherlands

(Received 24 April 1997)

Solid C_{60} can be intercalated with CO gas in a 1:1 ratio. The rovibrational motion of CO in these samples is studied as a function of temperature by IR and NMR spectroscopy. The observed spectra indicate a gradual transition from nearly free motion of CO at room temperature to hindered motion at low temperature, with only tunneling between symmetry equivalent orientations remaining. The observations are augmented by theory, and details on the local environment of the CO molecules are extracted. [S0031-9007(97)03839-8]

PACS numbers: 81.05.Tp, 31.70.Ks, 36.20.Ng, 76.60.–k

Solid C_{60} is a promising matrix for the storage of guest species, both inside and in between the cages. It consists of only one type of atoms, and the high molecular symmetry results in well-defined and uniform intercalation sites. For a detailed study of the guest-host interaction, the sparse spectral structure of the matrix in, for example, infrared (IR) and ^{13}C nuclear magnetic resonance (NMR) spectra is of advantage. In the face-centered cubic (fcc) lattice of C_{60}, two types of interstitial sites are available for intercalants, one large octahedral site and two smaller tetrahedral sites per C_{60} molecule [1]. The octahedral site is located at the center of the conventional cell of the fcc lattice. In the high temperature phase this site has O_h symmetry (crystal structure $Fm\bar{3}m$), whereas below the sc $\leftarrow$ fcc [sc (simple cubic)] ordering transition the symmetry of the site is reduced to S_6 (crystal structure $Pa\bar{3}$) [2]. With a lattice constant $a = 1.41$ nm and a C_{60} "van der Waals diameter" of 1.00 nm, it follows that this site can contain a sphere with a diameter of 0.41 nm. It has been reported that molecular oxygen and molecular hydrogen [3,4] as well as rare gas atoms [5] can be trapped in the octahedral sites via high pressure, high temperature synthesis, but no information on the dynamics of these trapped gases has become available so far.

Here we report data on the dynamics of CO intercalated in solid C_{60}. A CO molecule, with a "van der Waals length" of 0.44 nm [6], fits snugly in the octahedral site of the C_{60} lattice. The tetrahedral sites are much too small to contain a CO molecule. CO intercalated C_{60} samples are produced by exposing high purity polycrystalline C_{60} powder (Hoechst, "Super Gold Grade" C_{60}, purity $\geq$99.9%) or a thin film of C_{60} to CO at a temperature of 200 °C and a pressure of 10 MPa for about a day. Under these conditions samples with an almost 1:1 stoichiometry of $CO : C_{60}$ are obtained, resulting in CO densities in the solid equivalent to that of CO gas at 5 MPa pressure. These samples are stable under ambient conditions. On the order of a percent of the CO leaks out per day, while when put into vacuum at a temperature of 200 °C all CO is removed within a few minutes. It is spectroscopically confirmed that free CO molecules and pristine C_{60} are retrieved by the latter procedure.

For IR absorption experiments, 5 μm thick films of CO intercalated C_{60} on IR transparent substrates are used. Absorption spectra covering the 400–4000 cm^{-1} region are measured as a function of temperature with an experimental spectral resolution of 0.1 cm^{-1}. Reference spectra are measured on the C_{60} films prior to their exposure to CO. After intercalation with CO, a new spectral structure that is strongly temperature dependent is readily identified. In Fig. 1(b) the additional structure appearing in the 2000–2250 cm^{-1} region is shown for four different temperatures. The spectral features due to C_{60} (not shown) are hardly influenced both in position and in intensity by the presence of CO. Only a slight frequency shift, up to 0.5 cm^{-1}, is observed for some C_{60} modes.

For comparison, a spectrum of free CO molecules in the gas phase is shown in Fig. 1(a) while a spectrum of CO in an Ar matrix, where its rotational motion is completely blocked, is shown in Fig. 1(c). For CO in solid C_{60}, the broad spectral structure visible at room temperature gradually merges into a sharp resonance centered around 2124 cm^{-1} upon lowering the temperature. This resonance splits into at least two components upon approaching 0.6 K. The total integrated intensity of the CO related absorption is constant within a factor of 2 over the complete temperature range. There is no discontinuity in the appearance of the spectral structure associated with CO in crossing the rotational ordering sc $\leftarrow$ fcc phase transition of C_{60} [2]. The simultaneously measured C_{60} spectra change discontinuously in crossing this phase transition, bracketed between 230–260 K (pure C_{60}: 260 K [9]), in full accord with observations reported by others for pristine C_{60} [10].

The series of spectra shown in Fig. 1(b) indicates a transition from a situation in which the CO molecules have significant freedom to move to a situation in which this motion is strongly hindered. At high temperature the wings of the spectra resemble the envelope of the rotational structure of a free CO molecule. The center peak

 0031-9007/97/79(6)/1138(4)$10.00

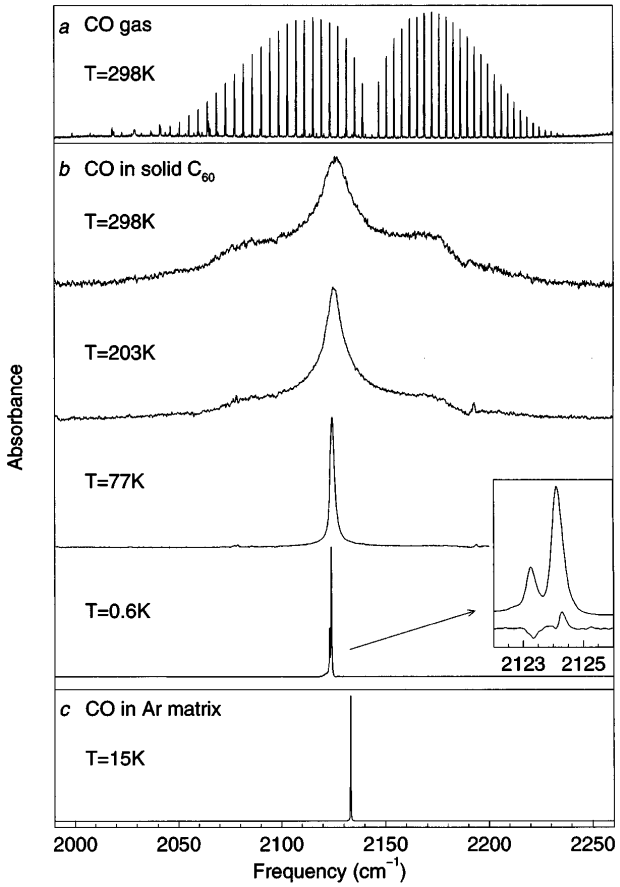

FIG. 1. Fourier transform infrared (FTIR) absorption spectra (Bruker IFS 66v/113v) of (a) CO gas at room temperature, (b) CO in the octahedral sites of the cubic C_{60} lattice for four different temperatures, and (c) CO in an Ar matrix at 15 K [7]. The weak structure appearing in the spectra about 2080 and 2190 cm^{-1} is caused by rather strong IR absorption bands that are intrinsic to C_{60} [8] and that are not completely corrected for by subtracting the reference spectra. At 0.6 K the resonance is split into two components at 2123.3 and 2124.1 cm^{-1} with a full width at half maximum of 0.35 cm^{-1}. In the lower trace of the inset the difference between the spectra recorded at 0.6 and 3.7 K is shown.

in the room temperature absorption spectrum is attributed to CO molecules that occupy states that are below the barrier for free rotation. At liquid nitrogen temperature the absorption spectrum resembles mostly that of CO fixed in a matrix. It is detailed below, however, that the observed splitting at 0.6 K indicates that, down to the lowest temperatures, quantum mechanical tunneling motion of CO occurs between symmetry equivalent orientations in the structured potential well.

Further information on the dynamics of CO in solid C_{60} and on the symmetry of the CO site is obtained from ^{13}C NMR spectroscopy. For the NMR experiments a 150 mg polycrystalline sample of C_{60} with natural isotopic abundance is intercalated with 99% ^{13}C enriched CO. Under magic angle spinning (MAS) conditions, two sharp resonances at 142.4 and 183.9 ppm are detected. These resonances can unambiguously be assigned to C_{60} (pure C_{60}: 143 ppm [11]) and CO (pure CO: 182.2 ppm [12]). From the intensity ratio of the two resonances in a fully relaxed spectrum it is concluded that approximately 15% of the octahedral sites are occupied in this particular sample. In other samples, in particular in the IR film samples, 100% of the octahedral sites could be filled. The less efficient filling of the present sample is attributed to the large size of the C_{60} crystallites and their short exposure time to CO. MAS spectra measured between 200 and 300 K reveal a single ^{13}CO resonance of constant linewidth and resonance frequency.

In contrast, the line shape of the ^{13}CO resonance from a static sample is strongly temperature dependent in this region, as shown in Fig. 2. At all temperatures shown, the width of the resonance is much smaller than the width of the chemical shift tensor of solid CO ($\delta_\perp - \delta_\parallel \approx 365 \pm 20$ ppm at 4.2 K [13]). At room temperature, a symmetric line centered around the isotropic chemical shift value is found. This is in agreement with the expectation of the rapid motion of CO on the NMR time scale in an environment with O_h symmetry, which averages the second-rank tensor of the chemical shift anisotropy to its isotropic value. At temperatures below that of the sc $\leftarrow$ fcc orientational ordering phase transition of C_{60}, the symmetry of the "octahedral" site is reduced to S_6. This lowering of the symmetry leads to a nonvanishing anisotropic contribution to the chemical shielding that is clearly reflected in the NMR line shape below 240 K. The experimental line shape at 200 K is described approximately by an axially symmetric chemical shift

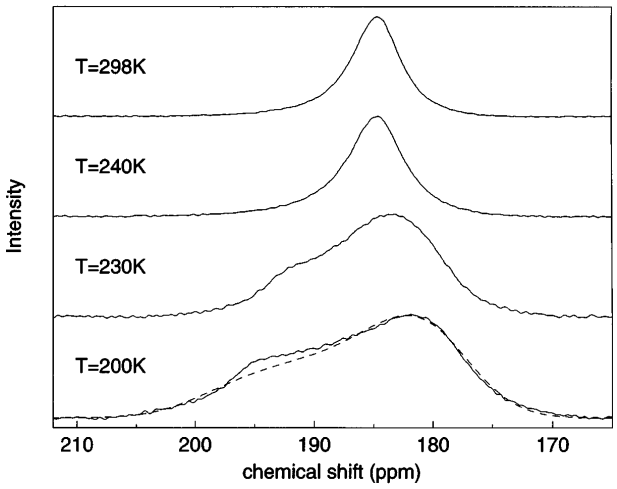

FIG. 2. ^{13}C NMR resonance of CO in a 150 mg CO intercalated polycrystalline C_{60} sample measured on a Bruker AM500 spectrometer under static conditions for various temperatures using a Doty probe. Each spectrum consists of 5000 scans taken at 6 s time intervals. The chemical shift is referenced to tetramethylsilane (TMS). For the pattern observed at 200 K, the best fit to an axially symmetric tensor with $(\delta_\perp - \delta_\parallel) = -20 \pm 1$ ppm, convoluted with a Gaussian line shape with 9 ppm FWHM, is shown as well (dashed). The intensity at high ppm values cannot be completely accounted for; a similar (unexplained) deviation has been found for solid CO [13].

tensor, in accordance with the expectation for a dynamically averaged tensor in a potential of S_6 symmetry. The observed tensor anisotropy of (-20 ± 1) ppm is considerably smaller than the static anisotropy of CO, indicating that considerable averaging still takes place.

Theoretical calculations are performed to aid in the interpretation of the experimental data. Rigid C_{60} molecules are positioned on an fcc lattice. Their orientation is taken either as the "major" or "minor" orientation that is experimentally found for C_{60} in the simple cubic $Pa\bar{3}$ low-temperature phase [1]. The potential felt by CO is due to the combined van der Waals interaction with the surrounding C_{60} molecules, and it does depend on the orientation of its six nearest-neighbor C_{60} molecules. The CO molecule is in a potential with S_6 symmetry only when all C_{60} molecules are in the same orientation. The interaction is described with the same atom-atom potential as used for endohedral $CO@C_{60}$ [6]. The five-dimensional (5D) bound states for a rigid CO molecule inside this potential are calculated; three of the dimensions refer to the motion of the center of mass of CO, while the other two dimensions describe the orientation of the CO axis.

The quantum mechanical method to compute the energy levels of CO inside this cavity is based on a discrete variable representation for the radial coordinate of the CO center of mass and an expansion of the angular wave functions in symmetry-adapted and coupled spherical harmonics [6]. It is important for the present study that this method includes the angular-radial coupling caused by the hindering potential of the cavity walls exactly and that it also describes large amplitude vibrations and hindered rotations of CO, with the inclusion of tunneling between multiple (equivalent) minima on the five-dimensional potential surface. From the energy levels and the corresponding wave functions, the frequencies and intensities of all the allowed dipole transitions are calculated, and the infrared spectrum is synthesized for different temperatures.

A three-dimensional (3D) equipotential surface for the position of the center of mass of CO with all C_{60} molecules in the major orientation, obtained by taking a cut through the five-dimensional potential surface for an optimized CO orientation, is shown in Fig. 3. There are eight minima present in the potential for the position of the CO center of mass, all being off-center. In these minima the CO points with the oxygen atom in between three C_{60} molecules towards the second nearest neighbors. The two equivalent (local) minima on the C_3-symmetry axis are approximately 30 cm^{-1} less deep than the six equivalent (global) minima along the three other cube diagonals. In contrast, with all C_{60} molecules in the minor orientation, the calculation predicts the minima on the C_3 axis to be the global minima. If we assume that in the 200–230 K range the C_{60} molecules rapidly interconvert between the major and the minor orientation, an effective potential that is a linear combination of the ones just described, and that still has

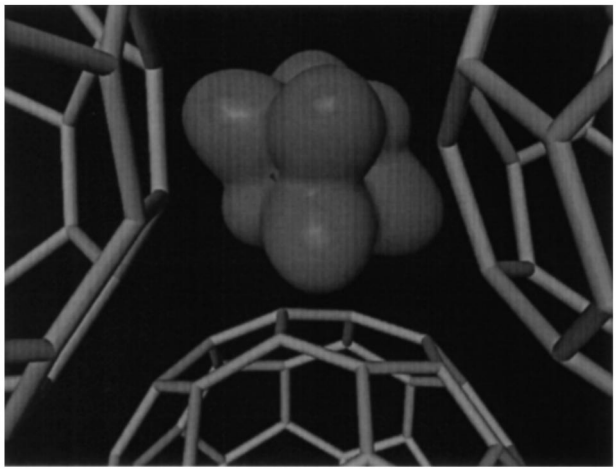

FIG. 3. A 3D equipotential cut (85 cm^{-1} above the global minima) through the 5D potential energy surface is shown, indicating the position of the center of mass of CO for an optimized CO orientation, with all C_{60} molecules in the major orientation. This potential has six global and two local minima along the cube diagonals.

S_6 symmetry, is sampled by the NMR measurements. In a simple model, the orientational distribution for the CO molecules described above may be replaced by the eight discrete minima. Then, the motionally averaged chemical shielding tensor [14] is the weighted sum of eight axially symmetric second-rank tensors, of which six and two, respectively, are symmetry equivalent. The principal values of all tensors may be assumed to be identical (supported by the appearance of a single CO resonance in the MAS spectrum) but the principal axes differ. A preferential population of the six equivalent minima leads to an averaged chemical shift tensor with an inverted sign of the asymmetry $(\delta_\perp - \delta_\parallel)$ with respect to the original tensor.

In Fig. 4 the observed IR spectrum of CO in solid C_{60} measured at 203 K is compared to the calculated IR spectrum. The calculation is done in S_6 symmetry, with all C_{60} molecules in the major orientation. For a true comparison with the experimental spectrum, a superposition of calculated spectra belonging to that of CO in sites with C_{60} molecules in random orientations has to be made. This will lead to a blurring of the sharp spectral structures in the calculated spectrum, bringing this in even better agreement with experiment.

Below liquid nitrogen temperature, the major and minor orientations of C_{60} are randomly frozen throughout the solid in a 5:1 ratio [15]. Under the assumption that this ratio is the same for C_{60} intercalated with CO, this leaves approximately one-third of the CO molecules surrounded solely by C_{60} molecules in the major orientation. These CO molecules are in a potential with six equivalent global minima, with a calculated tunnel splitting on the order of a cm^{-1}. In the IR spectrum this will result in two almost equally strong components separated by twice the tunnel splitting. The extra intensity in the high-frequency

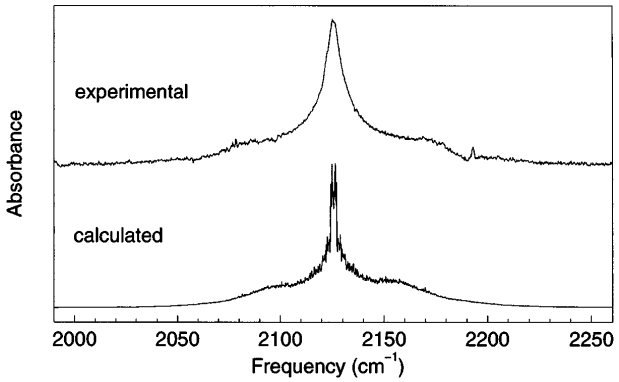

FIG. 4. Observed IR spectrum of CO in solid C_{60} at 203 K compared to the calculated IR spectrum. In the calculation a lattice parameter $a = 1.41$ nm is taken, and the orientation angle ϕ of the C_{60} molecules around their respective {111} axes (related according to $Pa\bar{3}$ symmetry) is taken as $\phi = 23.5°$ (major orientation). In the calculation, energy levels up to 600 cm^{-1} above the ground state level are included. The calculated spectrum is convoluted with a Gaussian with a full width at half maximum of 0.25 cm^{-1}.

component in the 0.6 K IR spectrum is attributed to the other two-thirds of the CO molecules that are in sites in which no measurable tunnel splitting is expected. The observed splitting of almost 1 cm^{-1} in the IR spectrum at low temperature is interpreted as the direct spectroscopic signature of quantum-mechanical tunneling motion of the CO molecule. This interpretation is substantiated by the observed intensity transfer from the low-frequency component to the high-frequency component in reducing the temperature from 3.7 K to 0.6 K, as shown in the difference spectrum in the inset of Fig. 1(b).

Small molecules *inside* fullerene cages have been suggested to form an ideal system for the study of nearly free molecular rotation in the solid, and experimental evidence for the motion of a scandium trimer inside a C_{82} fullerene cage has, for instance, been reported [16]. In addition, it has been pointed out that small polar molecules trapped inside the highly symmetric C_{60} cage might be considered the building blocks for an ideal electric dipolar lattice [17]. The results reported here indicate that samples in which small molecules are trapped in the octahedral sites of solid C_{60}, i.e., *in between* C_{60} molecules, samples that are much easier to produce, are equally interesting and promising and might show many of the characteristics, and enable many of the applications, anticipated for the corresponding endohedral species. In addition, it is demonstrated that molecules such as CO intercalated in fullerene samples are a very sensitive local probe of crystal structure and molecular orientation. It has also been shown here that gases can be efficiently stored in solid fullerene samples. The understanding of the guest-host interaction in a well-defined system as described here is a prerequisite for the understanding of gas storage in more complicated fullerene-related solids as, for instance, the recently reported storage of hydrogen in carbon nanotube material [18].

This work is part of the research program of the Stichting voor Fundamenteel Onderzoek der Materie (FOM), which is financially supported by the Nederlandse Organisatie voor Wetenschappelijk Onderzoek (NWO), and receives direct support from the NWO via PIONIER Grant No. 030-66-8g. We acknowledge helpful discussions with Professor S. van Smaalen.

[1] P. A. Heiney, J. Phys. Chem. Solids **53**, 1333 (1992).
[2] P. A. Heiney, J. E. Fischer, A. R. McGhie, W. J. Romanow, A. M. Denenstein, J. P. McCauley, Jr., A. B. Smith III, and D. E. Cox, Phys. Rev. Lett. **66**, 2911 (1991); R. Sachidanandam and A. B. Harris, Phys. Rev. Lett. **67**, 1467 (1991).
[3] R. A. Assink, J. E. Schirber, D. A. Loy, B. Morosin, and G. A. Carlson, J. Mater. Res. **7**, 2136 (1992).
[4] Z. Belahmer, P. Bernier, L. Firlej, J. M. Lambert, and M. Ribet, Phys. Rev. B **47**, 15 980 (1993).
[5] G. E. Gadd, P. J. Evans, D. J. Hurwood, J. Wood, S. Moricca, M. Blackford, M. Elcombe, S. Kennedy, and M. James, Chem. Phys. Lett. **261**, 221 (1996).
[6] E. H. T. Olthof, A. van der Avoird, and P. E. S. Wormer, J. Chem. Phys. **104**, 832 (1996).
[7] Y. Ogawara, A. Bruneau, and T. Kimura, Anal. Chem. **66**, 4354 (1994).
[8] K.-A. Wang, A. M. Rao, P. C. Eklund, M. S. Dresselhaus, and G. Dresselhaus, Phys. Rev. B **48**, 11 375 (1993).
[9] R. D. Johnson, C. S. Yannoni, H. C. Dorn, J. R. Salem, and D. S. Bethune, Science **255**, 1235 (1992).
[10] K. Kamarás, L. Akselrod, S. Roth, A. Mittelbach, W. Hönle, and H. G. von Schnering, Chem. Phys. Lett. **214**, 338 (1993).
[11] C. S. Yannoni, R. D. Johnson, G. Meijer, D. S. Bethune, and J. R. Salem, J. Phys. Chem. **95**, 9 (1991).
[12] A. J. Beeler, A. M. Orendt, D. M. Grant, P. W. Cutts, J. Michl, K. W. Zilm, J. W. Downing, J. C. Facelli, M. S. Schindler, and W. Kutzelnigg, J. Am. Chem. Soc. **106**, 7672 (1984).
[13] A. A. V. Gibson, T. A. Scott, and E. Fukushima, J. Magn. Res. **27**, 29 (1977). Note that in this publication the chemical shift scale is reversed compared to our Fig. 2.
[14] M. Mehring, *Principles of High Resolution NMR in Solids* (Springer, Berlin, 1983).
[15] W. I. F David, R. M. Ibberson, T. J. S. Dennis, J. P. Hare, and K. Prassides, Europhys. Lett. **18**, 219 (1992).
[16] P. H. M. van Loosdrecht, R. D. Johnson, M. S. de Vries, C.-H. Kiang, D. S. Bethune, H. C. Dorn, P. Burbank, and S. Stevenson, Phys. Rev. Lett. **73**, 3415 (1994).
[17] J. Cioslowski and A. Nanayakkara, Phys. Rev. Lett. **69**, 2871 (1992).
[18] A. C. Dillon, K. M. Jones, T. A. Bekkedahl, C. H. Kiang, D. S. Bethune, and M. J. Heben, Nature (London) **386**, 377 (1997).